CHEMPHYSCHEM

DOI: 10.1002/cphc.200700130

Impact of Bridging Units on the Dynamics of Photoinduced Charge Generation and Charge Recombination in Donor–Acceptor Dyads**

Antoine Van Vooren, Vincent Lemaur, Aijun Ye, David Beljonne, and Jérôme Cornil*[a]

We estimate, at a full quantum-chemical level, the various molecular parameters governing the rate of photoinduced charge generation and charge recombination in model organic structures containing a donor and an acceptor unit in view of the possible use of such systems in organic solar cells. The rate of through-space excitation dissociation, as predicted in the framework of the Marcus–Levich–Jortner theory, is found to be low in comparison to intramolecular decay processes when the donor and acceptor molecules are lying in a head-to-tail arrangement and high when the donor and acceptor molecules are superimposed in a cofacial arrangement. The charge separation rates for side-by-side donor–acceptor dyads are significantly increased by promoting through-bond interactions in covalently linked donor and acceptor units. This has motivated a detailed quantitative analysis of the influence of the nature, size, and conformation of the bridging moiety on the calculated transfer rates.

1. Introduction

Electron-transfer reactions are fundamental processes in many scientific fields.[1] In particular, they are responsible for the conversion of light into chemical energy in photosynthetic systems.[2] They also play a key role in the emerging field of organic photovoltaics, which aims at producing electricity at low cost and with a large conversion efficiency to fulfill the need for renewable sources of energy.[3,4]

An organic solar cell is fabricated by sandwiching an organic layer between two electrodes of different nature [typically, indium tin oxide (ITO) and aluminum]. The organic layer is made of two different materials: a π-electron-donating material (D) characterized by a low ionization potential and a π-electron-accepting material (A) characterized by a high electron affinity. The conversion of light into an electrical current relies on four successive steps:[3] 1) The incident photons are absorbed by the donor and/or acceptor units (D→D* and/or A→A*); in a simple one-electron picture, an electron is then promoted from the HOMO (highest occupied molecular orbital) to the LUMO (lowest unoccupied molecular orbital) of the excited compound to generate an electron–hole pair; these Coulombically bound species are particularly stable, with a binding energy on the order of a few tenths of an electronvolt,[5] owing to the low dielectric constants characteristic of organic materials. 2) The electron–hole pair diffuses to reach the interface between the donor and acceptor domains. 3) At the interface, the electron promoted into the LUMO level of the excited donor (L_D) is transferred to the lower-lying LUMO level of the acceptor (L_A) though a photoinduced electron transfer (PET) process, with the hole remaining on the donor (Figure 1). The same final charge-separated state (D^+A^-) is reached upon photoexcitation of the acceptor by a photoinduced hole (PHT) transfer from the HOMO level of the acceptor (H_A) to the HOMO level of the donor (H_D). In both cases, the dissociation is thermodynamically favorable if the energy gained during the transfer compensates the reduction of the binding energy of the intramolecular electron–hole pair.[6] 4) The generated charges escape from their mutual Coulomb attraction and migrate in opposite directions towards the electrodes, typically by hopping from molecule to molecule under the influence of the built-in potential.

The dynamics of electron-transfer processes strongly impact the overall performance of organic solar cells. A high conversion efficiency requires the electron–hole pair dissociation to be faster than any intramolecular radiative or nonradiative decay channel (with a rate generally around $10^9\ s^{-1}$). Moreover, the geminate charge carriers have to escape their mutual Coulomb attraction before a charge-recombination (CR) process to the ground state occurs by transferring the electron from the LUMO of the acceptor to the HOMO of the donor (Figure 1). Once separated, the charges are still subject to possible recombination mechanisms, which, according to the Langevin re-

[a] A. Van Vooren, Dr. V. Lemaur, Dr. A. Ye,[+] Dr. D. Beljonne, Dr. J. Cornil
Laboratory for Chemistry of Novel Materials
University of Mons-Hainaut
Place du Parc 20, B-7000 Mons (Belgium)
Fax: (+32) 65-373861
E-mail: Jerome@averell.umh.ac.be

[+] Current address:
Department of Chemistry
State University of New York at Buffalo
New York 14260-3000 (USA)

[**] A Quantum-Chemical Insight

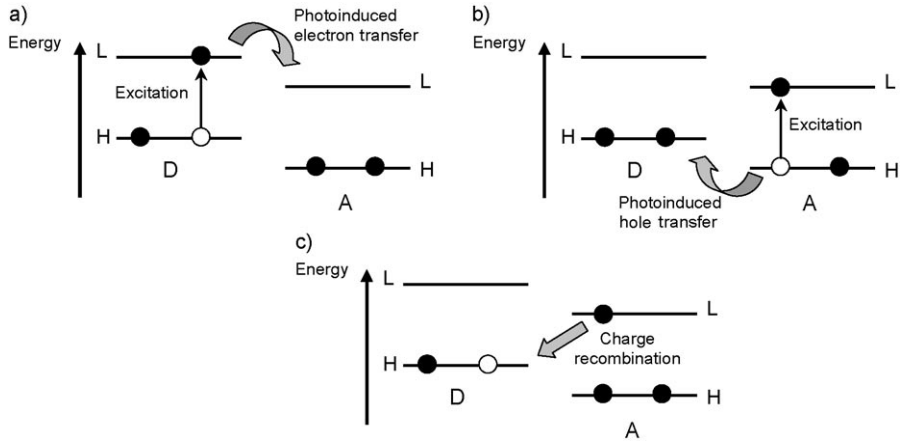

Figure 1. Energy diagram of a donor–acceptor (D--A) complex and representation of a) the photoinduced electron-transfer process; b) the photoinduced hole-transfer process; c) the charge-recombination process. ●, electrons; ○, holes; L = LUMO, H = HOMO.

combination model,[7] are less likely in the case of mobile charge carriers. The charge carriers can also yield triplet polaron pairs that decay into intramolecular triplet excited states.[8] These considerations have triggered a large number of experimental studies of charge generation and recombination dynamics in well-defined donor–acceptor complexes in solution.[2,9–14] In such model systems, the donor is generally bound covalently to the acceptor by means of a bridging (B) unit, thus implying that the dynamics are governed both by the nature of the D, B, and A units and by their relative positions (which are further modulated by the vibrations of the system[15]). However, it is not straightforward to assess the actual contribution of the bridge to the dynamics of the various processes in such structures.

At the theoretical level, the rate of an electron-transfer reaction can be estimated in the framework of Marcus theory and is expressed in the semiclassical limit as in Equation (1):[16]

$$k_{if} = \frac{2\pi}{\hbar}|V_{if}|^2 \frac{1}{\sqrt{4\pi\lambda k_B T}} \exp[-(\Delta G^\circ + \lambda)^2/4\lambda k_B T] \qquad (1)$$

where V_{if} represents the electronic coupling between the initial and final states, ΔG° is the free enthalpy of the reaction, and λ is the total reorganization energy that includes an internal (λ_i) and an external (λ_s) contribution. We have recently developed a theoretical procedure based on semiempirical Hartree–Fock approaches to evaluate all parameters entering the Marcus expression and hence the transfer rates without the need of experimental or fitted parameters.[17] This method offers a unique tool to investigate quantitatively on the basis of model systems the relationship between the relative position of the donor and acceptor units and the corresponding charge generation and recombination rates as well as the impact of bridging units. In this context, this approach is applied herein to a model system involving a pentacene molecule as the donor (that has been used in some organic solar cells[18,19]) and a pentacene molecule substituted by four cyano groups as the acceptor (chemical structures in Figures 2a and b). This donor–acceptor pair yields a driving force for exciton dissociation (on the order of 0.7–1 eV depending on the polarity of the solvent) of the same order of magnitude as that typically found for the supramolecular systems investigated experimentally;[9,14] the actual nature of the donor–acceptor units and of the surrounding medium has no major impact on the main conclusions drawn from this study.

Herein, we first compare the rate of charge generation and recombination when the donor and acceptor units are superimposed versus when they lie in the same plane. In the latter case, the results show that the electron–hole pair dissociation rate is low compared to the typical decay rate of intramolecular excitations, on the order of $10^9\ s^{-1}$ (the radiative decay rate in pentacene has been estimated to be around $10^8\ s^{-1}$).[20] This finding implies that the photoinduced charge transfer between one stack of donor molecules and an adjacent stack of nonbonded acceptor molecules is a relatively inefficient process. However, the calculations further illustrate that these rates can be significantly improved by covalently bridging the donor and acceptor units. To do so, we have connected here the two molecules by means of linear saturated and unsaturated hydrocarbon chains, and we have assessed the influence of the size and conformation of these chains. The electronic coupling associated with charge-transfer processes in bridged systems has been widely investigated at the theoretical level in cases where the donor and acceptor units are identical (see, for instance the reviews in refs. [21] and [22]) but much less often in systems presenting different moieties.[23–30] Moreover, the molecular parameters appearing in Equation (1) have been rarely

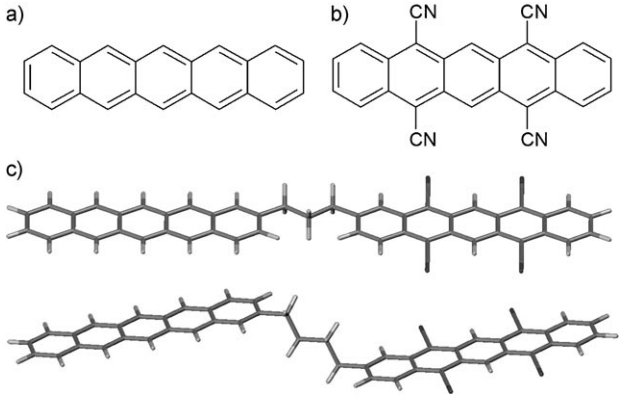

Figure 2. a) Chemical structure of the donor molecule. b) Chemical structure of the acceptor molecule. c) Structure of the D–B–A system with a planar bridge (top) and a bridge in a staircase geometry (bottom).

addressed in parallel to access a full theoretical estimate of the transfer rates, as it is the case herein.

2. Theoretical Methodology

We have optimized the geometry of the isolated donor and acceptor units in the relevant states (D, D^+, D*, A, A^-, and A*) with the semiempirical Hartree–Fock Austin Model 1[31] method coupled to a full configuration interaction scheme (AM1-CI), as implemented in the AMPAC package.[32] The size of the active space (typically 10–20 active orbitals) has been chosen in all instances to ensure the convergence of the geometric parameters. The saturated and unsaturated bridges have been introduced in an all-*trans* configuration without geometry optimization. The C–C and C–H bond lengths are fixed at 1.54 and 1.12 Å, respectively, for the saturated bridges and at 1.45 Å for single C–C bonds, 1.35 Å for double C–C bonds, and 1.10 Å for the C–H bonds in the polyenic bridges, as suggested by AM1 calculations on alkanes and butadiene. Two different structures have been considered in particular (Figure 2c): 1) a planar geometry for which the carbon atoms of the bridge are lying in the same plane as the pentacene molecular backbones; and 2) a staircase geometry for which the carbon atoms of the bridge are lying in a plane perpendicular to that defined by the pentacene molecular backbones.

In order to account for possible tunnelling effects across activation barriers that are neglected in the semiclassical limit, the transfer rates have been estimated with the Marcus–Levich–Jortner formalism that treats the intramolecular vibrational modes at a quantum-mechanical level. When considering that a single effective mode (with an energy $\hbar\omega$ set to 0.2 eV) assists the electron transfer, the corresponding expression is given by Equation (2):[33]

$$k_{if} = \frac{2\pi}{\hbar} V_{if}^2 \frac{1}{\sqrt{4\pi\lambda_s k_B T}} \sum_v e^{-S} \frac{S^v}{v!} \exp\left(-\frac{(\Delta G^\circ + \lambda_s + v\hbar\omega)^2}{4\lambda_s k_B T}\right) \quad (2)$$

where S the Huang–Rhys factor, is directly related to the internal reorganization energy ($S = \lambda_i/\hbar\omega$), and v refers to the number of the vibrational level.

The free enthalpy of the reaction ΔG° has been estimated as the difference between the energies of the initial and final states when neglecting entropy effects. ΔG° for the $D^*A \rightarrow D^+A^-$ process can be formulated as in Equation (3):

$$\Delta G^\circ = E(D^+) + E(A^-) - E(D^*) - E(A) + E_{Coulomb} \quad (3)$$

with [Eq. (4)]:

$$E_{Coulomb} = \frac{1}{4\pi\varepsilon_0\varepsilon_s}\left(\sum_{D^+}\sum_{A^-}\frac{q_{D^+}q_{A^-}}{r_{D^+A^-}} - \sum_{D^*}\sum_{A}\frac{q_{D^*}q_{A}}{r_{D^*A}}\right) \quad (4)$$

where $E(D^*)$, $E(D^+)$, $E(A)$, and $E(A^-)$ represent the total energies of the isolated donor in the equilibrium geometries of the lowest excited state and of the cationic state and the total energies of the isolated acceptor in the equilibrium geometries of the ground state and of the anionic state, respectively. The Coulomb term describes the change in the electrostatic interactions between the two molecules when going from the initial to the final state; this term is dominated by the contribution arising from the charge-separated state. q_D and q_A correspond to the Mulliken atomic charges on the donor and acceptor units, respectively, in their relevant states, and r_{DA} the separation between them. The choice of the simple Mulliken charge partitioning scheme is motivated by the fact that the amplitude of the Coulomb term in Equation (4) is hardly affected by the details of the charge distributions over the donor and acceptor units. The sum runs over all atoms of the two individual molecules. ε_s is the static dielectric constant of the medium; we have used the dielectric constant of tetrahydrofuran (THF; $\varepsilon_s = 7.52$), which is generally used as a good solvent for the characterization of supramolecular systems in solution. The total energies and atomic charges have been estimated on the basis of the frozen AM1-CI geometries, with an explicit account of the medium effects via the COSMO solvation model,[34] as implemented in AMPAC.[32] This approach has been found to yield driving forces in good quantitative agreement with corresponding experimental values.[35]

The internal reorganization energy λ_i mostly reflects the changes in the geometry of the donor and acceptor units between the two states. This parameter can be estimated as λ_{i1} corresponding to the difference between the energy of the reactants in the geometry characteristic of the products and that in their equilibrium geometry or as λ_{i2} corresponding to the difference between the energy of the products in the geometry characteristic of the reactants and that in their equilibrium geometry.[17] λ_{i1} is equal to λ_{i2} when the two potential energy surfaces describing the reactants and products have the same curvature; when this is not the case, λ_i is estimated as the average of λ_{i1} and λ_{i2}.[16] In the case of an electron–hole pair dissociation, the two terms can be written as Equations (5) and (6):

$$\lambda_{i1} = E^{D^*}_{geoD^+} + E^{A}_{geoA^-} - E^{D^*}_{geoD^*} - E^{A}_{geoA} \quad (5)$$

$$\lambda_{i2} = E^{D^+}_{geoD^*} + E^{A^-}_{geoA} - E^{D^+}_{geoD^+} - E^{A^-}_{geoA^-} \quad (6)$$

where $E^{D^+}_{geoD^*}$ represents the energy of the isolated positively charged donor in the geometry of the neutral molecule in its first singlet excited state, as calculated at the AM1-CI/COSMO level. λ_i does not depend on the relative position of the donor and acceptor units and is assumed to be unaffected by the presence of the bridge. Internal reorganization energies of 0.040 eV (0.009 eV for $D^* \leftrightarrow D^+$ and 0.031 eV for $A \leftrightarrow A^-$), 0.045 (0.044 eV for $D \leftrightarrow D^+$ and 0.001 eV for $A^* \leftrightarrow A^-$) and 0.075 eV (0.044 eV for $D \leftrightarrow D^+$ and 0.031 eV for $A \leftrightarrow A^-$) have been obtained for the PET, PHT, and CR processes, respectively. Small individual contributions indicate that the geometry of the molecule is very similar in the initial and final states. The calculated polaronic relaxation energy for pentacene ($\lambda_{rel} = E^{D^+}_{geoD} - E^{D^+}_{geoD^+}$) that appears within the CR process compares very well to the corresponding experimental value extracted from gas-phase

UPS (ultraviolet photoelectron spectroscopy) spectra (0.044 eV vs 0.050 eV[36]).

The external part of the reorganization energy λ_s reflects the inertial contribution to the response from the solvent molecules upon going from the initial to the final state.[16] It has been estimated by adapting the classical dielectric continuum model initially used by Marcus for electron-transfer reactions between spherical ions in solutions.[16] Our expression takes into account the atomic charge distribution over the donor and acceptor units [Eq. (7)]:

$$\lambda_s = \frac{1}{8\pi\varepsilon_0}\left(\frac{1}{R_D}+\frac{1}{R_A}-2\sum_D\sum_A\frac{q_D q_A}{r_{DA}}\right)\left(\frac{1}{\varepsilon_{opt}}-\frac{1}{\varepsilon_s}\right) \quad (7)$$

where ε_s is the static dielectric constant of the medium and ε_{opt} its optical dielectric constant ($\varepsilon_{opt}=1.98$ for THF). q_D and q_A are the atomic charges on the donor and acceptor units in the charge-separated state, respectively, as obtained at the AM1-CI/COSMO level. R_D (3.24 Å) and R_A (3.68 Å) are the effective radii of the donor and acceptor units estimated as the radius of the sphere having the same surface as the solvent-accessible surface of the molecule provided by COSMO.

The electronic coupling V_{if} reflects the strength of the interaction between the two states. When the donor and acceptor units are the same (i.e. in a self-exchange reaction), V_{if} is generally assimilated within a one-electron picture to a transfer integral related to charge-carrier transfer between two orbitals (i.e. between the HOMOs of the two units for hole transfer and between the LUMOs for electron transfer). The transfer integral is generally estimated within the Koopman approximation as half the splitting of the HOMO [LUMO] level in the neutral dimer for hole [electron] transfer between two identical molecules.[26,37–39] For sake of comparison, the transfer integrals for hole and electron transfer in the ground state (HT and ET) have been calculated hereafter for systems containing two pentacene molecules as D and A units, using the semiempirical Hartree–Fock INDO (intermediate neglect of differential overlap) Hamiltonian.[40] The same approach could be applied to a system with different D and A units by explicitly taking into account the energy difference between the HOMO/LUMO levels of the isolated molecules.[41] However, the evaluation can be severely hampered by electrostatic and polarization effects that lead to an offset between the electronic levels in the dimer prior to the interaction of the two units[42] (such effects are also operative in asymmetric dimers formed by two identical molecules); this can be corrected by promoting a full resonance between the two electronics levels with the help of an electric field applied along the charge-transfer direction.[24,43] Note that our theoretical procedure relies on two different semiempirical Hartree–Fock methods due to the fact that AM1 has been specifically parameterized to deal with geometric structures while INDO has been developed to describe spectroscopic properties suitably.

We have used two different approaches exploiting the INDO method to calculate V_{if} for the PET, PHT, and CR processes on the basis of the geometry of the reactants (D*/A for ET, D/A* for HT, and D^+/A^- for CR). The first approach is based on the two-state generalized Mulliken–Hush (GMH) formalism, which expresses the electronic coupling as given in Equation (8):[27,30,44–46]

$$V_{if} = \frac{\mu_{if}\Delta E_{if}}{\sqrt{(\Delta\mu_{if})^2+4(\mu_{if})^2}} \quad (8)$$

where ΔE_{if} is the energy difference, $\Delta\mu_{if}$ the variation in the permanent dipole, and μ_{if} the transition dipole moment (projected along the $\Delta\mu_{if}$ direction) between the initial and final states. Since all states of interest have a dominant one-electron character in our model system (D*A is mostly described by a $H_D\rightarrow L_D$ transition, DA* by a $H_L\rightarrow L_L$ transition, and D^+A^- by a $H_D\rightarrow L_A$ transition), the three parameters have been calculated by means of INDO calculations coupled to a single configuration scheme (SCI) incorporating, besides the ground-state determinant, the dominant configuration describing the involved excited states (i.e. D*A and D^+A^- for the photoinduced electron transfer, DA* and D^+A^- for the photoinduced hole transfer, and only D^+A^- for the charge-recombination process). Introducing additional configurations would generate additional states, which could interact with the states of interest and rule out the use of a two-state model.[47,48] We stress that INDO has been found to provide couplings that compare very well to corresponding ab initio Hartree–Fock values.[49,50]

When the two states involved in the process under consideration have a dominant one-electron character and vary by a single orbital, as it is the case here, another approach to estimate V_{if} is to compute directly the transfer integral between the two orbitals (i.e. between L_D and L_A for the photoinduced electron transfer, H_D and H_A for the photoinduced hole transfer, and between L_A and H_D for the charge-recombination process). The coupling between molecular orbitals ϕ_1 and ϕ_2 (belonging to molecules i and j, respectively) can be recast in an atomic orbital basis set as given in Equation (9):

$$V_{if} = \langle\phi_1|h|\phi_2\rangle = \sum_\mu\sum_\nu C_{1\mu}C_{2\nu}\langle\chi_\mu|h|\chi_\nu\rangle \quad (9)$$

where $C_{1\mu}$ and $C_{2\nu}$ correspond to the LCAO (linear combination of atomic orbitals) coefficients of the atomic orbitals χ_μ and χ_ν in the molecular orbitals ϕ_1 and ϕ_2, respectively. The matrix element $<\chi_\mu|h|\chi_\nu>$ is implemented in the INDO method as Equation (10):

$$\langle\chi_\mu|h|\chi_\nu\rangle = \frac{1}{2}(\beta_A+\beta_B)\bar{S}_{\mu\nu} \quad (10)$$

where β_A and β_B are parameters that depend on the nature of atoms A and B, $\bar{S}_{\mu\nu}$ is the overlap factor between the atomic orbitals χ_μ and χ_ν, corrected by empirical factors.[40]

We have applied the two different approaches to the calculation of the electronic coupling associated with charge generation ($D^*A\rightarrow D^+A^-$) in a dimer, where the D and A molecules are aligned along their molecular axis, with a distance between their centers of mass of 17 Å. The couplings are found to very similar (0.78 cm^{-1} with the direct method and 0.72 cm^{-1} with GMH). We have also applied a static electric field (with an am-

plitude up to $10^7\,V\,cm^{-1}$) along the charge-transfer direction to tune the location of the charge-transfer state and assess the impact on the electronic coupling; this electric field reflects in a first approximation an increase in the solvent polarity, since both modifications stabilize charge-transfer states. Applying an electric field up to $10^7\,V\,cm^{-1}$ shifts the energy of the charge-transfer state from 3 eV down to 0.5 eV. Yet, the application of the electric field hardly changes the amplitude of the transfer integral obtained by the direct method (reduction by only 2% over the range of applied electric fields). This small variation arises from the fact that the orbitals get slightly polarized over the molecule when the electric field is increased, thus reducing the electronic density in the overlapping region. In contrast, the coupling provided by the GMH approach displays strong and irregular variations. In particular, a sharp peak is observed around $10^6\,V\,cm^{-1}$, leading to electronic couplings as high as 300 cm^{-1} (Figure 3). This peak is observed when the LUMO

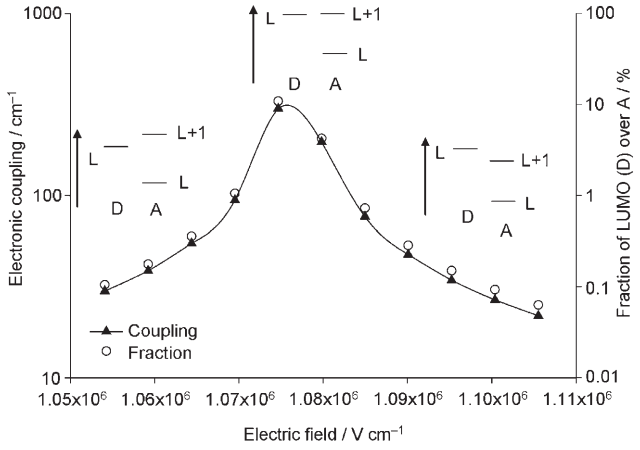

Figure 3. Evolution of the delocalization of the LUMO of the donor over the acceptor (○, %) and of the electronic coupling associated with the photoinduced electron transfer as estimated with GMH (▲, cm^{-1}) as a function of the amplitude of the electric field in a dimer where the D and A molecules are aligned along their molecular axis, with a distance between their centers of mass of 17 Å. The energy-level diagrams schematically depict the relative energies of the relevant orbitals at different electric fields; L = LUMO.

level of the donor is in resonance with the LUMO + 1 level of the acceptor. This situation promotes a delocalization of the LUMO level of the donor over the acceptor and is accompanied by a significant increase in the transition dipole moment appearing in the expression of the electronic coupling in Equation (8); this is further evidenced in Figure 3 by the field evolution of the extent of delocalization of L_D over the acceptor (estimated as the sum of the squares of the LCAO coefficients of L_D over the atoms of the acceptor unit). In view of the very weak couplings calculated from the direct method, this delocalization is likely to be left when accounting for the vibrational dynamics of the molecules and their environment and thus appears as an artifact of the GMH approach.[51] We are thus led to the conclusion that the two-state GMH formalism can provide strongly overestimated couplings when an accidental resonance between electronic levels of the donor and acceptor units occurs. We have checked that all couplings provided hereafter are not deeply affected by such delocalization effects.

3. Results and Discussion

We first consider two model structures where the donor and acceptor molecules are exactly superimposed or are aligned in the same plane. We report in Figure 4 the evolution of the cal-

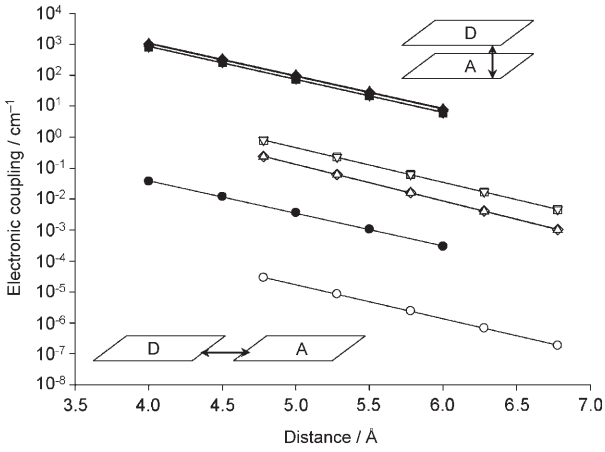

Figure 4. Distance dependence of the calculated electronic couplings for photoinduced electron (□, ■) and hole (◇, ◆) transfer, charge recombination (○, ●), and ground-state hole (△, ▲) and electron (▽, ▼) transfer processes. Filled symbols correspond to superimposed structures and open symbols to aligned structures.

culated electronic coupling for the photoinduced electron- and hole-transfer processes and for the charge-recombination process as a function of the intermolecular separation in the superimposed structures and of the distance separating the terminal carbon atoms in the aligned structures. Figure 4 also collects the transfer integrals obtained for holes and electrons when the D and A units are both a pentacene molecule. In all cases, the electronic coupling has been calculated from the direct evaluation of the relevant transfer integral. The results show for all processes an exponential decrease of the electronic coupling with the distance [Eq. (11)]:

$$V_{if} = V_0 \exp(-\beta_V d) \qquad (11)$$

where β_V is the decay factor characterizing the distance dependence of the electronic coupling; β_V should be as small as possible to allow for charge-transfer processes at long distances. This behavior is rationalized by the fact that the strength of the interaction reflects the degree of overlap between the π-atomic orbitals, whose wavefunctions decrease exponentially with increasing distance from the nuclei. Similar couplings are obtained for the photoinduced electron and hole transfer in the D–A complex and the ground-state electron and hole transfer in the D–D complex; this result is rationalized by the fact that the LCAO pattern of the frontier orbitals of pentacene

is weakly perturbed upon cyano substitution. In the following, we will no longer consider ground-state hole- and electron-transfer processes in systems with two pentacene molecules.

The electronic coupling for the charge-recombination process is lower than the charge separation by up to four orders of magnitudes in both structures. The amplitude of the CR electronic coupling is actually related to the degree of electronic overlap between the H_D and L_A levels. Since the H_D and L_A levels have different parities, there is full compensation between the bonding versus antibonding interactions in the overlapping region of the superimposed structure, which translates into virtually zero coupling (Figure 5). The LCAO patterns of the two molecular orbitals (MOs) also, for similar symmetry reasons, lead to a vanishingly small coupling in the aligned structures. In contrast, the MOs involved in the other processes have the same symmetry, thus promoting larger electronic couplings. Such symmetry constraints are often broken when the relative position of the donor and acceptor units is modulated.[17] The electronic couplings are systematically smaller (by about two to three orders of magnitude) in the aligned structures than in the superimposed structures; this effect is intuitively understood by the fact that the molecules are only interacting through their two terminal carbon atoms. The slightly larger coupling calculated for electron transfer is once again driven by the shape of the orbitals. As a matter of fact, Figure 6 illustrates that the interaction between the LUMO orbitals is fully bonding in the overlapping region, while there is a mixing of bonding and antibonding interactions for the HOMO levels.

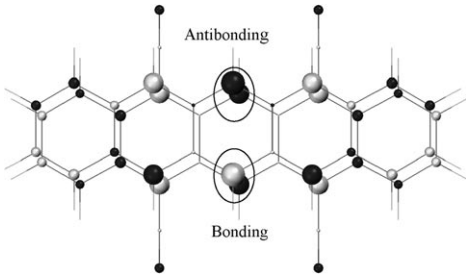

Figure 5. Shape of the H_D and L_A levels showing the full compensation of bonding versus antibonding interactions in the superimposed structure. The size and color of the spheres are representative of the amplitude and sign of the LCAO coefficients, respectively.

The rates estimated for the various processes when inserting the calculated V_{if}, λ_i, λ_s, and ΔG° values into Equation (2) are plotted in Figure 7 as a function of the intermolecular distance for both the cofacial and the aligned structure. In all cases, the transfer rate can be fitted to a single exponential decay when the distance is varied, as expected from the exponential dependence of the electronic coupling. Table 1 collects the β decay value associated with the transfer rate for each process and twice the β_V value associated with the electronic coupling [in view of the square dependence in Eq. (2)]. The close similarity between β and $2\beta_V$ demonstrates that the distance dependence of the transfer rate is mostly driven by the electronic coupling; the difference between β and $2\beta_V$ originates from the distance dependence of the Coulomb terms appearing in λ_s and ΔG°. The aligned structures provide the closest match between β and $2\beta_V$, since these parameters do not fluctuate very much in the range of separation between the centers of mass that we have considered. In contrast, the evolution is much more pronounced at the shorter distances found in the superimposed structures.

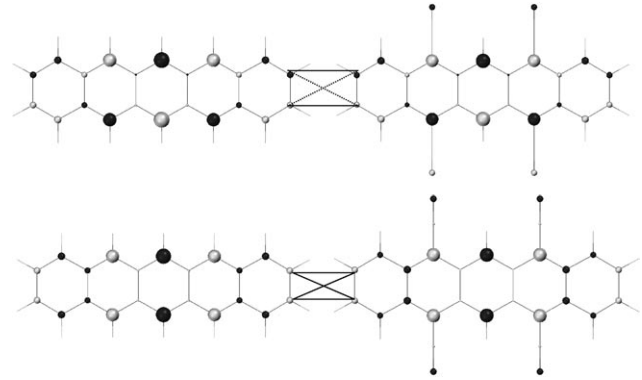

Figure 6. Shape of the frontier electronic levels of the D and A units showing that the interaction between the LUMO levels (bottom) is fully bonding in the overlapping region, while the interaction between the HOMO levels (top) displays a mixing of bonding and antibonding interactions. The size and color of the spheres are representative of the amplitude and sign of the LCAO coefficients.

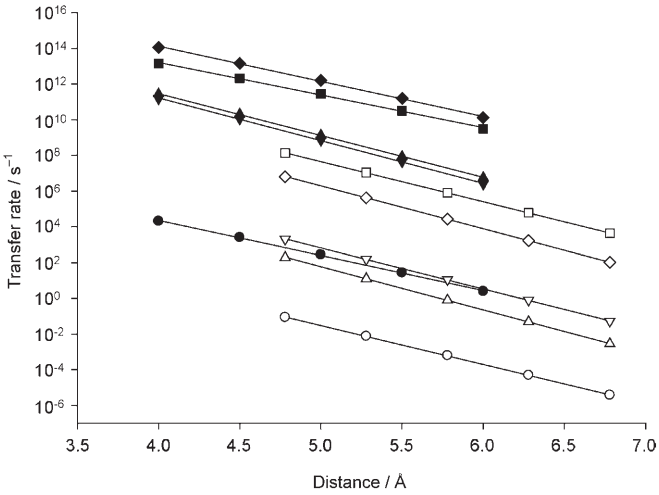

Figure 7. Distance dependence of the calculated transfer rates for photoinduced electron (□, ■) and hole (◇, ◆) transfer, charge recombination (○, ●), and ground-state hole (△, ▲) and electron (▽, ▼) transfer processes. Filled symbols correspond to superimposed structures and open symbols to aligned structures.

For both structures, the largest transfer rates are calculated for the PHT and PET processes; the rates for ground-state hole and electron transfer are smaller, since in those cases we have not accounted for a possible driving force induced by the application of a static electric field ($\Delta G^\circ = 0$) that would shift the rate towards the maximum of the Marcus parabola. The smallest transfer rate is obtained for the recombination process,

Table 1. Decay factors associated with the transfer rate (β) and the electronic coupling (β_V) for the various processes in cofacial and aligned structures.

Structure	Process	β [Å^{-1}]	$2\beta_V$ [Å^{-1}]
Cofacial	ET	4.20	4.91
	HT	4.53	4.86
	CR	4.51	4.84
	hole transport	5.41	4.87
	electron transport	5.52	4.91
Aligned	PET	5.18	5.15
	PHT	5.53	5.44
	CR	5.02	5.05
	HT	5.57	5.44
	ET	5.27	5.15

which is driven mostly by the small associated electronic coupling. Strikingly, the aligned structures yield, whatever the process, a rate much lower than the typical radiative decay rate of an excitation on a conjugated molecule,[20] except for in the case of small molecular separations. This finding indicates that electron–hole pair dissociation cannot compete with intramolecular processes in solar cells for supramolecular architectures in which the donor and acceptor units are in the same molecular plane. This is the case for adjacent stacks of donor and acceptor units, which are attractive because they promote good charge-transport properties along one-dimensional columns, especially when the separation between molecules is large owing to the presence of substituents. In contrast, the rates are sufficiently high to allow for efficient charge generation in the cofacial structures, although the absolute values are expected to be modulated by slight fluctuations in the geometric arrangement.[17]

The previous results have motivated us to introduce a bridge between the donor and the acceptor in the aligned structures to allow for through-bond electron transfer in addition to the through-space contribution considered so far. Improvements in the electronic coupling between a donor and acceptor unit upon introduction of a saturated bridge have been documented in several experimental[12,15,33,49,52,53] and theoretical[24–31] studies. Our work builds on this knowledge and adds a new contribution by introducing a theoretical approach that provides quantitative estimates of the transfer rates; this method allows us in turn to assess, in model and actual structures, the influence of several parameters (such as the bridge size and conformation) that cannot be easily accessed at the experimental level.

Figure 8 shows the evolution of the PET, PHT, and CR electronic couplings (Figure 8a) and rates (Figure 8b) obtained with the GMH approach as a function of the number of carbon atoms in a saturated bridge for both the planar and staircase geometries; note that only the GMH approach is applicable when the donor and acceptor units are covalently bound. The electronic couplings for the unbridged systems with the donor and acceptor units lying in exactly the same position are at least three orders of magnitude lower. The exponential decay of the electronic coupling (and thus of the rate) with distance is maintained upon introduction of the bridge; however, the

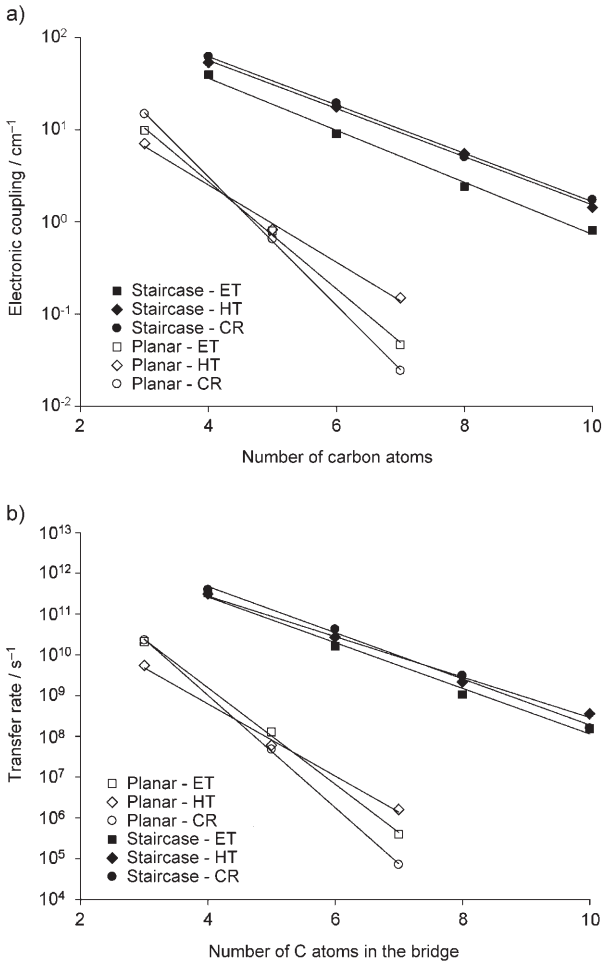

Figure 8. Evolution of a) the electronic coupling and b) the transfer rate for the photoinduced electron (□, ■) and hole (◇, ◆) transfer and charge-recombination (○, ●) processes as a function of the number of carbon atoms in the saturated bridge in both the staircase and planar geometries. Filled symbols correspond to staircase structures and open symbols to planar structures.

electronic couplings are significantly enhanced and the β decay values (almost equal to $2\beta_V$ in the aligned structures) strongly reduced. Table 2 collects the β and $2\beta_V$ values (as well as the corresponding values expressed per number of carbon atoms in the bridge) for the three processes for the two different geometries of the bridge. The large electronic couplings and smaller β values (around 1.2–1.4 Å^{-1}) calculated for electron–hole pair dissociation in the staircase geometry allow for fast charge generation in systems where the donor and acceptor units are separated by a large distance; this effect might prove very attractive for solar cells, since the generated charges are less weakly bound by Coulomb interactions and could thus easily separate before recombining, to yield free carriers. Note, however, that the rates for charge generation and charge recombination are comparable in the presence of the saturated bridge, which thus lifts the symmetry constraints associated with through-space transfer. Such symmetry constraints are expected to be recovered if the two pentacene derivatives are connected by a double-strand bridge made of

Table 2. Decay factors (β in Å^{-1} and per carbon atom) for the ET, HT, and CR processes upon introduction of a saturated bridge in both the planar and staircase geometries.

Structure	Process	β [Å^{-1}/per carbon]	$2\beta_V$ [Å^{-1}/per carbon]
Planar	PET	2.16/2.72	2.13/2.68
	PHT	1.62/2.04	1.53/1.93
	CR	2.52/3.17	2.54/3.21
Staircase	PET	0.97/1.22	0.98/1.23
	PHT	0.90/1.13	0.95/1.19
	CR	0.91/1.15	0.84/1.05

two parallel saturated chains like in norbornyl bridges.[54] On the other hand, the improvement brought by the planar bridge still appears to be too low for charge generation to compete efficiently with intramolecular processes (note that the large variations in the β values among the three processes are attributed to through-space contributions that are still active in the planar geometry); the rate is further deteriorated when cutting the bridge to mimic a complex in which the donor and acceptor units are substituted by saturated chains that are in contact. The β values calculated for the PET process with the bridge in the staircase geometry are slightly larger than those reported experimentally (0.75–0.98 Å^{-1})[21] for double-strand saturated hydrocarbon bridges displaying a similar conformation.

We have further analyzed the influence of the conformation of the bridge by evaluating the evolution of the PET rate as a function of the number of carbon atoms in the saturated bridge when modulating the torsion angle between the plane defined by the carbon atoms of the bridge and the molecular planes of the pentacene backbones between 0 and 90°, (Figure 9). The evolution of the β_V values extracted from an exponential fit of these results as a function of the torsion angle is plotted separately in Figure 10. Note that fitting the curves with a single exponential decay is an approximation, since the β_V values are likely to be weakly bridge-size dependent,[22] and

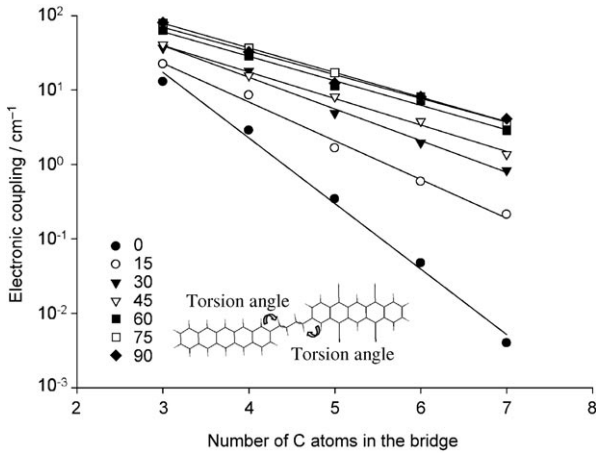

Figure 9. Evolution of the electronic coupling for the PET process as a function of the number of carbon atoms in the saturated bridge for different torsion angles between the D–B and B–A units.

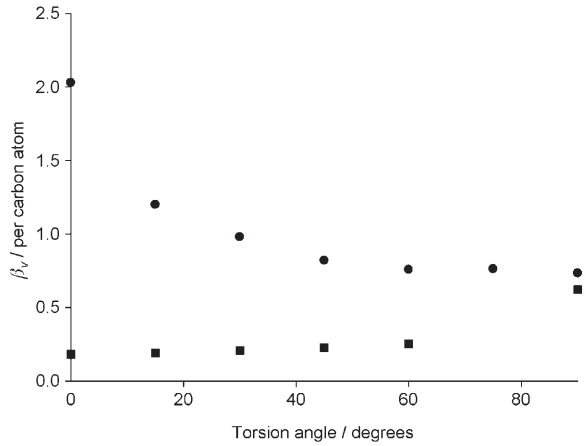

Figure 10. Evolution of β_V (per carbon atom) as a function of the torsion angle between the donor/acceptor units and the bridging unit for the saturated chain (●) and the polyenic segment (■).

since the results might be slightly affected by delocalization effects in the GMH approach. The β_V values do not change significantly at large torsion angles (1.31 Å^{-1} and 1.64 Å^{-1} for torsion angles of 90 and 45°, respectively) and increase when going towards small torsion angles. Similarly, the electronic couplings are large and slightly reduced when departing from 90° but drop significantly when reaching small angles. The amplitude of the electronic couplings and β_V values can be better understood on the basis of the McConnell model developed in a tight-binding formalism.[22,49,55] In this framework, the electronic coupling can be expressed as in Equation (12):

$$V_{if} = \frac{V_{DB}V_{BA}}{\Delta}\left(\frac{\nu}{\Delta}\right)^{m-1} \quad (12)$$

where m is the number of identical units in the bridge, ν the transfer integral between the repeating units of the bridge, Δ the energy gap between the frontier electronic levels of D and A with respect to the bridge orbitals (an average value should be considered when D and A are different), and V_{DB} and V_{BA} the transfer integrals between the orbital of the first repeating unit of the bridge that assists the transfer and the π-orbital on the connected atom of D and A, respectively; this implies that the bridge should be attached to an atom bearing significant electron density in the relevant molecular orbitals. When $\nu/\Delta \ll 1$, as is the case with saturated bridges, V_{if} decreases exponentially as a function of the distance between D and A with a decay factor given by Equation (13):

$$\beta_V = \ln\left|\frac{\Delta}{\nu}\right| \quad (13)$$

The amplitude of V_{DB} and V_{AB} increases as a function of the sine of the torsion angle, since the largest interaction is promoted at 90° (i.e. in the staircase geometry) when the σ orbitals of the C–C bonds of the bridge are almost parallel to the π orbitals of the pentacene molecules (Figure 1). For instance, V_{DB} and V_{AB} are reduced by a factor $\sqrt{2}/2$ going from 90 to 45°, thus implying from Equation (12) that the electronic coupling

is in turn reduced by a factor of two, in full agreement with the theoretical data. The evolution of β_V originates from a change in the nature of the bridge orbitals promoting the through-bond transfer as a function of the torsion angle. As a matter of fact, whereas the π orbitals of the pentacene molecules are most strongly coupled to the σ orbitals of the C–C bonds of the bridge at 90°, this interaction is fully cancelled at 0°, where the electronic overlap vanishes for symmetry reasons; it is actually the σ orbitals associated with the C–H bonds that assist the transfer in the planar geometry. Since the transfer integral v between σ orbitals associated with C–C bonds is larger than that associated with C–H bonds (Δ is not expected to vary significantly among the σ orbitals), the β_V value is smaller in the former case according to Equation (13), in full agreement with our theoretical results. The two sets of σ orbitals (i.e. those associated with the C–C or the C–H bonds) are active for intermediate torsion angles, and the coupling with the C–C bonds dominates until small angles are reached. When a DBA system has an equilibrium structure that does not allow for efficient PET or PHT processes, the vibrational dynamics can thus prove useful by promoting faster rates via the modulation of the torsion angles, which has been referred to as conformational gating.[15] To date, this issue has not often been addressed, and it clearly deserves particular attention in future experimental and theoretical studies.

We have reported in Figure 11 the electronic couplings as a function of the torsion angle when replacing the saturated bridge by a polyenic segment; the corresponding β_V values are reported in Figure 10 (we have not incorporated the value obtained for 75°, since large fluctuations are observed in the electronic couplings; such fluctuations are wiped out at small angles since the couplings become much stronger). The comparison of the β_V values calculated for polyenic bridges to corresponding experimental β values (with $\beta \approx 2\beta_V$) is not straightforward, since the latter are strongly system-dependent. However, our theoretical results ($2\beta_V = 0.30$–0.38 Å^{-1} between 0 and 60°) lie in the range of the experimental values reported for conjugated bridges ($\beta = 0.04$–0.4 Å^{-1}).[21] At small angles, the polyenic bridge generates electronic couplings (and hence transfer rates) larger than the highest values obtained with the saturated chain at 90° (523.2 cm^{-1} for four carbon atoms in the polyenic segment at 0° compared to 39.4 cm^{-1} for four carbon atoms in the saturated chains at 90°). This is rationalized by the fact that the π orbitals of the bridge are coupled significantly to the π orbitals of the donor and acceptor units at small angles and by the significant reduction in the energy gap Δ between the relevant orbitals [see Eq. (12)]; this effect is also accompanied by a significant reduction of the β_V value (down to 0.18 per carbon atom), in full consistency with Equation (13). In the case of the polyenic segment, the β_V value increases going from 0 to 90°, in contrast to the evolution prevailing for the saturated chain. This trend is again explained by a change in the nature of the bridge orbitals assisting the transfer, that is, from π orbitals to σ C–C orbitals, when going from 0 to 90°. This analysis is further supported by the fact that the β_V values obtained for the saturated versus polyenic bridges converge towards the same value around 90°.

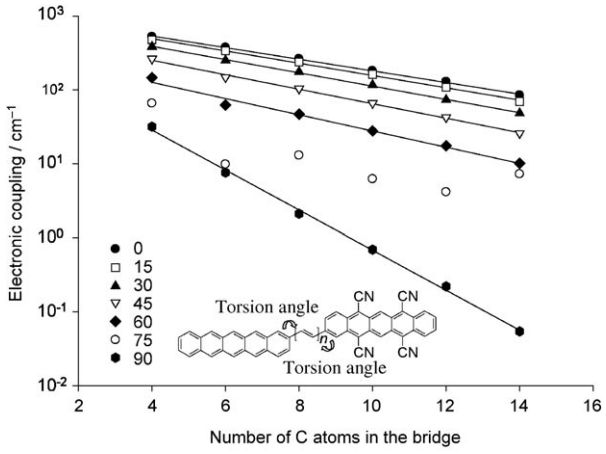

Figure 11. Evolution of the electronic coupling for the PET process as a function of the number of carbon atoms in the polyenic bridge for different torsion angles between the D–B and B–A units.

4. Conclusions

We have estimated at a quantitative level the rates of photoinduced charge generation and charge recombination in model organic donor–acceptor structures, in view of the possible use of such systems in organic solar cells This task has been accomplished by first computing the key molecular parameters at a quantum-chemical level and then inserting them into a rate expression derived from Marcus theory. The rate of photoinduced charge generation is quite low when the donor and acceptor units are lying in the same molecular plane. Thus, charge generation cannot efficiently compete with the intramolecular decay channels of the generated excitations. The charge generation and recombination rates are significantly increased by covalently connecting the donor and acceptor units though a bridging unit. When saturated hydrocarbon chains are introduced, the rate is maximized for a given chain length when the σ C–C orbitals of the bridge are lying parallel to the π orbitals of the donor and acceptor moieties. In contrast, charge transfer is optimized with polyenic spacers when the overlap between the π orbitals of the bridge and those of the donor and acceptor units is maximized. In both cases, the rate typically decreases exponentially with the size of the bridge, with a decay factor β reduced to 0.18 per carbon atom with the polyenic bridging units. The present results are of general applicability and demonstrate the interest of inserting bridging units in the donor–acceptor blends used in organic solar cells in order to allow for 1) charge transfer between adjacent stacks of donor and acceptor units; and 2) long-range charge-transfer processes that limit the Coulomb attraction between the generated charges in the final state and hence favor the generation of free charge carriers.

Acknowledgements

The work in Mons has been supported by the Belgian Federal Government "Interuniversity Attraction Pole in Supramolecular Chemistry and Catalysis, PAI 5/3", the European Integrated Project project NAIMO (NMP4-CT-2004-500355), and the Belgian National Fund for Scientific Research (FNRS/FRFC). J.C. and D.B. are FNRS Research Associates; A.V.V. acknowledges a grant from Fonds pour la Formation à la Recherche dans l'Industrie et dans l'Agriculture (FRIA).

Keywords: donor–acceptor systems · electron transfer · organic materials · quantum chemistry · solar cells

[1] P. F. Barbara, T. J. Meyer, M. A. Ratner, *J. Phys. Chem.* **1996**, *100*, 13148.
[2] M. R. Wasielewski, *Chem. Rev.* **1992**, *92*, 435.
[3] C. J. Brabec, N. S. Sariciftci, J. C. Hummelen, *Adv. Funct. Mater.* **2001**, *11*, 15.
[4] S. Sun, N. S. Sariciftci, *Organic Photovoltaics: Mechanisms, Materials, and Devices*, Marcel Dekker, New York, **2005**.
[5] I. G. Hill, A. Kahn, Z. G. Soos, R. A. Pascal, *Chem. Phys. Lett.* **2000**, *327*, 181.
[6] J. J. M. Halls, J. Cornil, D. A. dos Santos, R. Silbey, D. H. Hwang, A. B. Holmes, J. L. Brédas, R. H. Friend, *Phys. Rev. B* **1999**, *60*, 5721.
[7] V. D. Mihailtechi, L. J. A. Koster, J. C. Hummelen, P. W. M. Blom, *Phys. Rev. Lett.* **2004**, *93*, 216601.
[8] T. Offermans, P. A. van Hal, M. M. Koetse, S. C. J. Meskers, R. A. J. Janssen, *Phys. Rev. B* **2005**, *72*, 045213.
[9] E. E. Neuteboom, S. C. J. Meskers, P. A. van Hal, J. K. J. van Duren, E. W. Meijer, R. A. J. Janssen, H. Dupin, G. Pourtois, J. Cornil, R. Lazzaroni, J. L. Brédas, D. Beljonne, *J. Am. Chem. Soc.* **2003**, *125*, 8625.
[10] R. T. Hayes, M. R. Wasielewski, D. Gosztola, *J. Am. Chem. Soc.* **2000**, *122*, 5563.
[11] W. B. Davis, M. A. Ratner, M. R. Wasielewski, *Chem. Phys.* **2002**, *281*, 333.
[12] W. D. Oosterbaan, C. Koper, T. W. Braam, F. J. Hoogesteger, J. J. Piet, B. A. J. Jansen, C. A. van Walree, H. J. van Ramesdonk, M. Goes, J. W. Verhoeven, W. Schuddeboom, J. M. Warman, L. W. Jenneskens, *J. Phys. Chem. A* **2003**, *107*, 3612.
[13] J. W. Verhoeven, *Adv. Chem. Phys.* **1999**, *106*, 603.
[14] E. H. A. Beckers, S. C. J. Meskers, A. P. H. J. Schenning, Z. Chen, F. Würthner, R. Janssen, *J. Phys. Chem. A* **2004**, *108*, 6933.
[15] W. B. Davis, M. A. Ratner, M. R. Wasielewski, *J. Am. Chem. Soc.* **2001**, *123*, 7877.
[16] R. A. Marcus, *J. Chem. Phys.* **1965**, *43*, 679.
[17] V. Lemaur, M. Steel, D. Beljonne, J. L. Brédas, J. Cornil, *J. Am. Chem. Soc.* **2005**, *127*, 6077.
[18] S. Yoo, B. Dormercq, B. Kippelen, *J. Appl. Phys.* **2005**, *97*, 103706.
[19] A. K. Pandey, K. N. N. Unni, J. M. Nunzi, *Thin Solid Films* **2006**, *511–512*, 529.
[20] N. Nijegorodov, V. Ramachandran, D. P. Winkoun, *Spectrochim. Acta Part A* **1997**, *53*, 1813.
[21] M. N. Paddon-Row, *Aust. J. Chem.* **2003**, *56*, 729.
[22] K. D. Jordan, M. N. Paddon-Row, *Chem. Rev.* **1992**, *92*, 395.
[23] A. H. A. Clayton, K. P. Ghiggino; G. J. Wilson, M. N. Paddon-Row, *J. Phys. Chem.* **1993**, *97*, 7962.
[24] A. A. Voityuk, N. Rösch, M. Bixon, J. Jortner, *J. Phys. Chem. B* **2000**, *104*, 9740.
[25] M. Braga, S. Larsson, *J. Phys. Chem.* **1993**, *97*, 8929.
[26] I. Filatov, S. Larsson, *Chem. Phys.* **2002**, *284*, 575.
[27] J. Zheng, Y. K. Kang, M. J. Thieren, D. N. Beratan, *J. Am. Chem. Soc.* **2005**, *127*, 11303.
[28] M. B. Zimmt, D. H. Waldeck, *J. Phys. Chem. A* **2003**, *107*, 3580.
[29] A. Troisi, M. A. Ratner, M. B. Zimmt, *J. Am. Chem. Soc.* **2004**, *126*, 2215.
[30] X. Gao, S. Tang, W. Zhou, *Chem. Phys. Lett.* **2006**, *429*, 538.
[31] M. J. S. Dewar, E. G. Zoebisch, E. F. Healy, J. J. P. Stewary, *J. Am. Chem. Soc.* **1985**, *107*, 3902.
[32] AMPAC 6.55, Semichem, Shawnee, KS, **1997**.
[33] M. Bixon, J. Jortner, *Adv. Chem. Phys.* **1999**, *106*, 35.
[34] A. Klamt, G. J. Schüürmann, *J. Chem. Soc. Perk. T* **1993**, *2*, 799.
[35] G. Pourtois, D. Beljonne, J. Cornil, M. A. Ratner, J. L. Brédas, *J. Am. Chem. Soc.* **2002**, *124*, 4436.
[36] V. Coropceanu, M. Malagoli, D. A. da Silva Filho, N. E. Gruhn, T. G. Bill, J. L. Brédas, *Phys. Rev. Lett.* **2002**, *89*, 275503.
[37] M. N. Paddon-Row, M. J. Shephard, *J. Am. Chem. Soc.* **1997**, *119*, 5355.
[38] J. L. Brédas, D. Beljonne, V. Coropceanu, J. Cornil, *Chem. Rev.* **2004**, *104*, 4971.
[39] V. Balaji, K. D. Jordan, M. N. Paddon-Row, H. K. Patney, *J. Am. Chem. Soc.* **1987**, *109*, 6957.
[40] J. Ridley, M. C. Zerner, *Theor. Chim. Acta* **1973**, *32*, 111.
[41] J. Cornil, J. Ph. Calbert, J. L. Brédas, *J. Am. Chem. Soc.* **2001**, *123*, 1250.
[42] E. F. Valeev, V. Coropceanu, D. A. da Silva Filho, S. Salman, J.-L. Brédas, *J. Am. Chem. Soc.* **2006**, *128*, 9882.
[43] T. R. Prytkova, I. V. Kurnikov, D. N. Beratan, *J. Phys. Chem. B* **2005**, *109*, 1618.
[44] R. J. Cave, M. D. Newton, *Chem. Phys. Lett.* **1996**, *249*, 15.
[45] R. J. Cave, M. D. Newton, *J. Chem. Phys.* **1997**, *106*, 9213.
[46] R. J. Cave, M. D. Newton, K. Kumar, M. B. Zimmt, *J. Phys. Chem.* **1995**, *99*, 17501.
[47] M. Rust, J. Lappe, R. J. Cave, *J. Phys. Chem. A* **2002**, *106*, 3930.
[48] A. A. Voityuk, *Chem. Phys. Lett.* **2006**, *422*, 25.
[49] M. D. Newton, *Chem. Rev.* **1991**, *91*, 767.
[50] A. A. Voityuk, *Chem. Phys. Lett.* **2006**, *427*, 177.
[51] A. Troisi, G. Orlandi, *Phys. Rev. Lett.* **2006**, *96*, 086601.
[52] R. H. Goldsmith, L. E. Sinks, R. F. Kelley, L. J. Betzen, W. Liu, E. A. Weiss, M. A. Ratner, M. R. Wasielewski, *Proc. Natl. Acad. Sci. USA* **2005**, *102*, 3540.
[53] M. Liu, D. H. Waldeck, A. M. Olivier, N. J. Head, M. N. Paddon-Row, *J. Am. Chem. Soc.* **2004**, *126*, 10778.
[54] G. A. Jones, M. N. Paddon-Row, B. K. Carpenter, P. Piotrowiak, *J. Phys. Chem. A* **2002**, *106*, 5011.
[55] M. P. Eng, B. Albinsson, *Angew. Chem.* **2006**, *118*, 5754; *Angew. Chem. Int. Ed.* **2006**, *45*, 5626.

Received: February 21, 2007
Published online on April 23, 2007

